

Immunological mimicry of PrP^C–PrP^{Sc} interactions: antibody-induced PrP misfolding

Li Li¹, Will Guest^{1,2}, Alan Huang¹, Steven S. Plotkin²
and Neil R. Cashman^{1,3}

¹Brain Research Centre, The University of British Columbia, 2211
Wesbrook Mall, Vancouver, BC, Canada V6T 2B5 and ²Department
of Physics and Astronomy, The University of British Columbia, 6224
Agricultural Road, Vancouver, BC, Canada V6T 1Z1

³To whom correspondence should be addressed.
E-mail: neil.cashman@vch.ca

Prion diseases are associated with the conversion of cellular prion protein (PrP^C) to an abnormal protease-resistant conformational isoform (PrP^{Sc}) by template-directed conversion. The interaction between PrP^C and PrP^{Sc} is mediated by specific sites which have been mapped to six putative ‘binding and conversion domains’ (PrP-BCD) through peptide and antibody competition studies. Monoclonal antibodies (mAbs) directed against the bityrosine motif Tyr-Tyr-Arg (YYR) specifically recognize PrP^{Sc} and other misfolded PrP species. Here, we report that select bead-bound PrP-BCD mAbs induce exposure of bityrosine epitopes on mouse brain PrP. By competition immunoprecipitation, we show that PrP-BCD mAb-induced bityrosine exposure occurs at α -helices 1 and 3. However, PrP-BCD mAb-induced PrP^C misfolding is not accompanied by β -sheet dissociation, a key event in PrP^C conversion to PrP^{Sc}, and is not associated with acquisition of protease resistance, or the capacity to recruit additional molecules of PrP. Our data suggest that mAb mimics of the physical interaction of PrP^C with PrP^{Sc} can induce unfolding of specific PrP domains, but that subsequent processes (including the energetically unfavorable β -sheet dissociation) effect isoform conversion in prion disease.

Keywords: binding and conversion domains/misfolding/
monoclonal antibody/prion

Introduction

Prions are the infectious agents of the transmissible spongiform encephalopathies, which are thought to propagate on a post-translational level without requiring agent-specific nucleic acids for propagation (Riesner *et al.*, 1993). Infectivity is thought to reside in an abnormal conformational isoform (generically designated PrP^{Sc}) of the ubiquitous normal cellular prion protein (PrP^C), by a process known as ‘template directed conversion’ (Griffith, 1967; Prusiner, 1982, 1998). PrP^C can also be converted *in vitro* by contact with PrP^{Sc} (Kocisko *et al.*, 1994; Bessen *et al.*, 1995), and conversion can be promoted by serial sonication in protein misfolding cyclic amplification (Saborio *et al.*, 2001), or by incubation-shaking methodologies (Zou and Cashman, 2002; Atarashi *et al.*, 2007). Infectious PrP isoforms are generally resistant to protease digestion, and possess high β -sheet content, unlike the α -helix-rich PrP^C (Caughey *et al.*, 1991; Pan *et al.*, 1993; Safar *et al.*, 1993).

The mechanics of template-directed conversion are unknown, stymied by the lack of an atomic level structure for PrP^{Sc}, primarily due to its insoluble and aggregated state (Caughey *et al.*, 1995, 1997), and the apparent lack of discrete ultrastructure (Meyer *et al.*, 1986). In contrast, a regular ultrastructure has been observed in the protease-resistant core of PrP^{Sc} (PrP 27–30) subjected to high concentrations of non-denaturing detergents, designated scrapie-associated fibrils or prion rods (Merz *et al.*, 1981, 1983; Prusiner *et al.*, 1983; Meyer *et al.*, 1986). Two-dimensional crystals of prion rods display an apparent trimeric structure by transmission EM, compatible with a parallel left-handed β -helical fold (Wille *et al.*, 2002, 2007; Govaerts *et al.*, 2004). A plausible ‘spiral model’ for PrP^{Sc} has also been proposed from molecular dynamics simulation (Alonso *et al.*, 2001; DeMarco and Daggett, 2004, 2007), which may be more consistent with experimental data than the β -helix model (DeMarco *et al.*, 2006). A general criticism of these models is the assumption that multimers are passively recruited from ‘building blocks’ of PrP subunits misfolded prior to exposure to PrP^{Sc}, thus not adequately capturing the active process of template-directed conversion.

We have generated prion-specific mAbs (Paramithiotis *et al.*, 2003), which are useful to constrain models of PrP^{Sc} and which we also exploit in this study to provide insight into template-directed conversion. On the basis of the biophysical detection of Tyr exposure at the molecular surface of β -sheet-refolded recombinant PrP, mAbs were developed against a free YYR peptide, a motif present in β -strand 2 and α -helix 1 (Paramithiotis *et al.*, 2003), and later against 5-mers and 7-mers comprising YYR plus residues flanking β -strand 2 (‘ β -strand expanded epitope’, Cashman, unpublished). YYR and β -strand expanded mAbs specifically immunoprecipitate PrP^{Sc} from prion-infected tissues in humans, cattle, sheep and rodents, but not normal tissues, and bind to the surface of scrapie-infected follicular dendritic cells, but not normal cells (Paramithiotis *et al.*, 2003). Soluble PrP isoform-nonspecific mAb 6H4 (recognizing the YYR and flanking residues of α helix 1) did not cross-compete YYR mAb binding to PrP^{Sc} (Paramithiotis *et al.*, 2003), confirming that the ‘relevant’ PrP^{Sc}-specific YYR is β -strand 2. These data would suggest that PrP β -sheet dissociation is a necessary prerequisite to prion protein conversion in disease. However, simple denaturation of PrP^C by chaotropes or pH extremes is accompanied by YYR mAb recognition of bityrosine motifs in α -helices 1 and 3 (which lacks a terminal arginine).

We have reasoned that binding to PrP^{Sc} by PrP^C would be mediated through specific motifs of PrP^C. Indeed, competition experiments with PrP peptides and/or monoclonal antibodies (mAbs) have defined 6 PrP binding–conversion domains (PrP-BCDs; Fig. 1): PrP-BCD1 (human codons ~90–111; Peretz *et al.*, 2001; Moroncini *et al.*, 2004), PrP-BCD2 (~119–136; Chabry *et al.*, 1998, 1999), PrP-BCD3 (~136–157; Chabry *et al.*, 1998, 1999; Enari *et al.*, 2001; Heppner *et al.*, 2001; Peretz *et al.*, 2001;



Fig. 1. Illustration of PrP-BCDs and their cognate mAbs.

Moroncini *et al.*, 2004), PrP-BCD4 (~166–178; Horiuchi *et al.*, 2001) and PrP-BCD5 (200–223; Horiuchi and Caughey, 1999; Horiuchi *et al.*, 2001). More recently, using an elegant ‘shotgun’ grafted antibody approach by Williamson, PrP-BCD1 and PrP-BCD3 have been confirmed, and PrP-BCD6 has been defined at the PrP N-terminus (Solforsosi *et al.*, 2007). We have now developed a novel immunological system to mimic the interaction of PrP^C to PrP^{Sc}, in order to dissect the molecular events triggered by isoform binding in a controlled and non-infectious system. We have assembled or generated a series of defined mAbs whose epitopes overlap with, or are immediately adjacent to, the PrP-BCDs detailed above. We reasoned that mAbs, as relatively massive molecules, could be faithful mimics of multimeric PrP^{Sc} molecular surface binding. These mAbs (Fig. 1) are 6D11, reacting to PrP-BCD1 (Pankiewicz *et al.*, 2006; Sassoon *et al.*, 2005); SAF61 and 6H4, with overlapping reactivity to PrP-BCD3 (Korth *et al.*, 1997; Mouillet-Richard *et al.*, 2000); POM5, reacting to PrP-BCD4 (Polymenidou *et al.*, 2005); POM10, reacting to PrP-BCD5 (Polymenidou *et al.*, 2005) and 8B4, reacting to PrP-BCD6 (Li *et al.*, 2000; Pan *et al.*, 2004).

Materials and methods

Reagents and antibodies

Monoclonal anti-prion mAb 8B4 was purchased from Alicon AG (Schlieren, Switzerland), 6D11 was purchased from Signet Laboratory (Dedham, MA, USA) and SAF61 was purchased from Cayman Chemical (Ann Arbor, MI, USA). POM mAbs (mouse IgG1) were purchased from Dr A. Aguzzi (Zurich, Switzerland). Mouse IgG1 isotype control mAb was purchased from Sigma Aldrich (Oakville, ON, Canada). Protease K (PK) was purchased from Invitrogen (Burlington, ON, Canada). All other chemicals were purchased from Sigma Aldrich unless specified otherwise. 4C2 is a mouse IgG1 mAb directed against a 7-mer epitope of the β -strand 2 YYR plus two flanking residues C- and N-terminally (Paramithiotis *et al.*, 2003). 4C2 was conjugated to Alexa 488 by AbLab in the University of British Columbia (The Biomedical Research Centre, UBC Vancouver, BC, Canada).

Brain tissues and homogenate preparation

Tg20 mice (Fischer *et al.*, 1996) were obtained from the European Mouse Mutant Archive (Neuherberg/Munich, Germany) and bred in isolators. Mouse brain tissues were frozen immediately after collection and stored at -80°C . Ten percent (w/v) brain homogenates were prepared in homogenization buffer [100 mM NaCl, 10 mM EDTA, 0.5% Nonidet P-40 (NP-40), 0.5% sodium deoxycholate, 10 mM Tris-HCl, pH 7.5] as previously described (Li *et al.*, 2007).

mAb-beads coupling

Anti-PrP mAbs at 50 $\mu\text{g}/\text{ml}$ were coupled to magnetic Dynabeads (Invitrogen) as described (Zou and Cashman, 2002), and stored in PBS at 4°C .

Flow cytometric analysis

Flow cytometry was performed on mAb-conjugated beads, in which 10 μl beads were incubated with 1 μl 10% brain homogenate at room temperature for 3 h. The immune complexed beads were washed $3\times$ with PBS and subsequently reacted with biotin-conjugated PrP mAbs 3 h at room temperature. After two washes, beads were incubated for 30 min at room temperature with FITC-streptavidin or Cy5-streptavidin (Jackson ImmunoResearch, West Grove, PA, USA). Bead fluorescence was assayed using a FACS-Calibur flow cytometer (BD, San Jose, CA, USA), the fluorescence intensity of FITC and Alexa 488 were detected by FL1 channel and Cy5 was detected by FL4 channel. In mAb competition assays, mAb beads were incubated with BH for 3 h at room temperature to induce PrP misfolding, following by incubation of 4C2-Alexa 488 with soluble Abs (SAF61 and POM10) overnight. The mean of fluorescence intensity was determined using Flow Jo Software.

PK digestion and immunoblotting

To study the profile of PK sensitivity for mAb-induced misfolded PrP, the samples were incubated for 1 h at 37°C with different concentrations of PK ranging from 0 to 100 $\mu\text{g}/\text{ml}$, followed by immunoblot analysis as described (Zou and Cashman, 2002).

Unfolding energy estimation

The unfolding free energies of the bityrosine motifs were calculated as described previously (Guest *et al.*, 2008). Briefly, enthalpy changes were derived from all-atom molecular dynamics simulations, solvation entropy changes from changes in solvent-accessible surface area and configurational entropy changes from an analytic diffusion model of the unfolded peptide chain.

Results

PrP-Bcd mAbs induce exposure of bityrosine epitopes in mouse brain PrP

In a program designed to molecularly dissect the process of template-directed conversion, we reacted mouse brain homogenate PrP^C with bead-coupled mAbs directed against PrP-BCD domains (Fig. 1), and monitored the acquisition of PrP bityrosine immunoreactivity using fluorescein-labeled 4C2 mAb. Experiments were conducted with Tg20 mouse brain homogenates, which overexpress the mouse *Prnp* gene, to maximize sensitivity of the assays. We obtained PrP-BCD mAbs 8B4, 6D11, SAF61, POM5 and POM10, which were

all demonstrated to react with natively structured PrP^C by conventional immunoprecipitation–immunoblotting, and by flow cytometry of the neuroblastoma-motor neuron hybrid cell line NSC34 (not shown). However, in our magnetic bead-flow cytometry system, only 8B4 (human codons 37–44), 6D11 (codons 89–109) and POM10 (codons 219–222) were found to appreciably bind mouse brain PrP^C, as detected by a second primary anti-PrP mAb (Fig. 2, and not shown). When compared with negative controls (beads only, beads coupled to BSA and beads coupled to irrelevant IgG; not shown), incubation of PrP with bead-coupled 8B4, 6D11 and POM10 mAbs also induced YY(R) exposure (Fig. 2). Although the acquisition of 4C2 immunoreactivity was time-dependent, virtually all bityrosine exposure was induced within the first hour of incubation, suggesting PrP-BCD mAb-induced misfolding is a rapid process.

8B4-induced bityrosine exposure

Given the prominent 4C2 immunoreactivity of PrP induced by 8B4 beads, we utilized this mAb to determine which PrP bityrosine motifs are exposed by 8B4 induction, by performing competition experiments with soluble unlabeled antibodies (Fig. 3). No competition of Alexa 488-labeled 4C2 binding was observed using soluble unlabeled IgG1 isotype control mAb, indicating that PrP-BCD mAb competition results were specific. Binding of Alexa 488-labeled 4C2 was efficiently competed with unlabeled 4C2, consistent with the recognized epitope(s) comprising an authentic antibody–antigen interaction. When soluble mAbs were co-incubated with labeled 4C2 (Fig. 3a), efficient competition was observed with unlabeled SAF61, reactive with an epitope on α -helix 1 which includes a YYR epitope, but not with unlabeled POM 10, a C-terminal reactive mAb overlapping

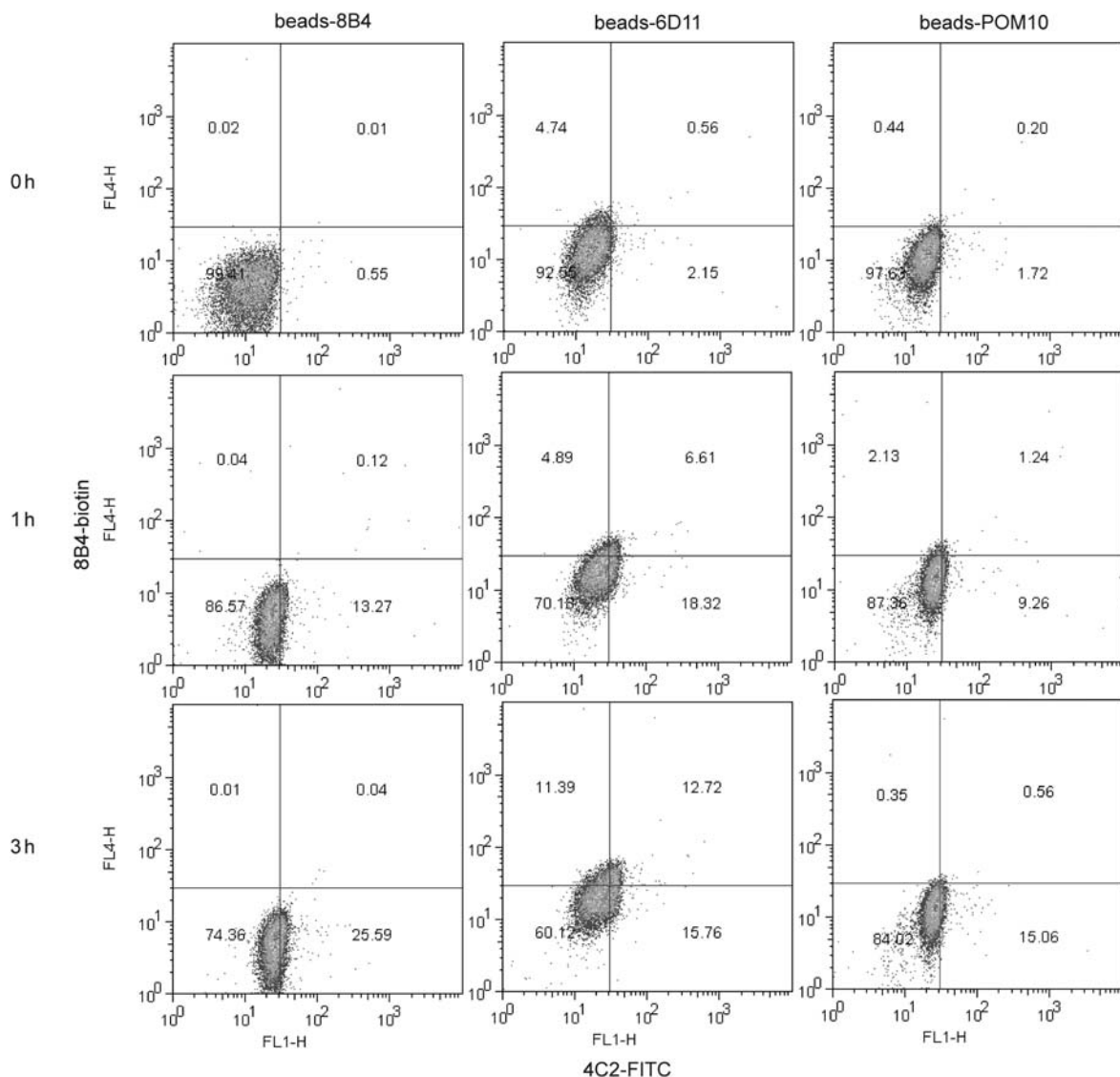


Fig. 2. Induction of misfolded PrP by various PrP-BCD mAbs as detected by the exposure of the YY motifs with 4C2-FITC antibody. Flow cytometric quadrant analysis of FITC-labeled 4C2 fluorescence intensity (FL1, X-axis) versus the biotinylated 8B4 fluorescence intensity (FL4, Y-axis). Lower left quadrant, 4C2-8B4-negative beads; lower right quadrant, 4C2-positive-8B4-negative beads; upper left quadrant, 4C2-negative-8B4-positive beads; upper right quadrant, 4C2-8B4-positive beads. Numbering refers to the percentage of each quadrant beads. Bead-bound PrP was incubated with fluorescein-coupled soluble mAbs for 30 min to determine the exposure of YY(R) motifs by FL1 channel (X-axis), with nearly all the immunoreactivity being generated in the first hour of bead incubation. 8B4-biotin mAb demonstrates bound PrP for 6D11 and POM10 mAb beads detected with FL4 channel (Y-axis), but binding of PrP to 8B4 beads was demonstrated with fluorescein-coupled 6D11 because of competition between bead-bound 8B4 and soluble 8B4.

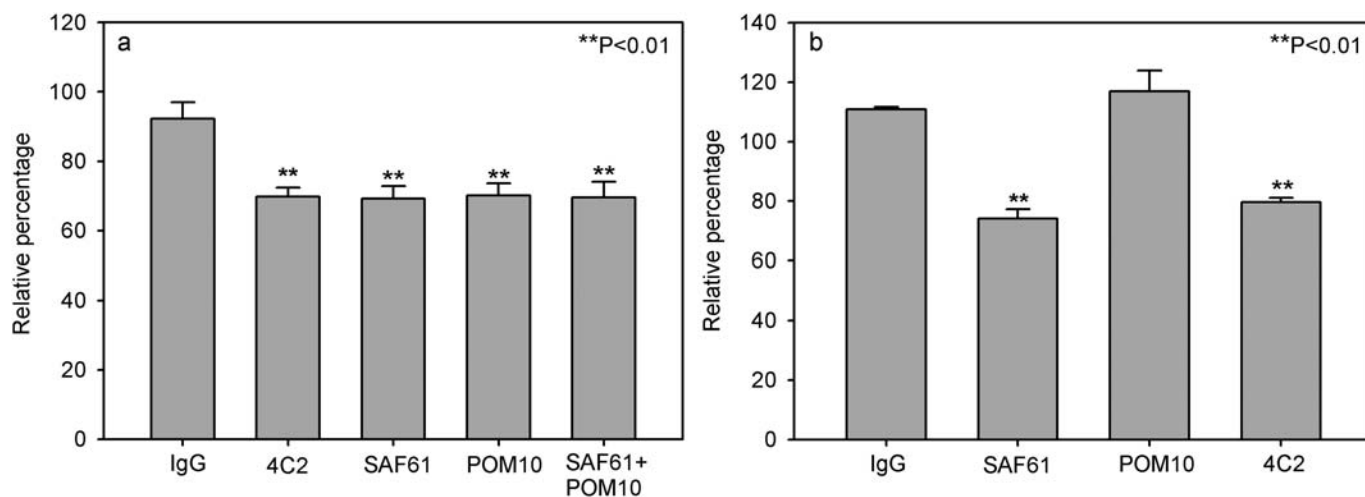


Fig. 3. Mapping YY motifs exposed by 8B4 mAb binding, by relative competition of fluorescence intensity of 4C2-Alexa 488 detected by flow cytometry. (a) 8B4 bead-induced PrP misfolding followed by simultaneous competition between soluble PrP mAbs and 4C2-Alexa 488; (b) 8B4 bead-induced PrP misfolding, followed by incubation with 300 μ g/ml soluble Abs SAF61, POM10 and 4C2 overnight at 4°C and detection by 4C2-Alexa 488.

with a bityrosine sequence (YYQR in mice). However, when saturating concentrations of mAbs were incubated overnight with 8B4-induced PrP (Fig. 3b), 4C2 binding inhibition was observed by both SAF61 and POM10, suggesting that consolidation of POM10 binding obviated 4C2 access to the C-terminal bityrosine. Notably, co-competition experiments with soluble unlabeled 4C2 in combination with SAF61 and POM10 did not indicate additional 4C2 binding sites beyond α -helices 1 and 3 (Fig. 3b), suggesting a lack of exposure of the PrP β -strand 2 YYR in 8B4 induction. This finding was supported by additional experiments using β -strand-2-specific mAbs (kindly provided by Dr Avi Chakrabarty, University of Toronto, Canada), and a β -strand 1 mAb developed in our laboratory (not shown).

8B4 misfolded PrP does not resemble PrP^{Sc}

Although incubation of PrP with bead-bound PrP-BCD mAbs induces exposure of bityrosine motifs consistent with subtle loss of structure of the PrP^C globular domain, β -sheet dissociation characteristic of PrP^{Sc} was not observed. To determine if other PrP^{Sc} properties might be induced in our system, we tested whether 8B4-induced PrP might trigger the recruitment of additional PrP molecules (Fig. 4a), and the acquisition of protease resistance (Fig. 4b). Tg20 brain homogenates were incubated with various PrP-BCD mAb-coupled beads, followed by detection with the same population of PrP-biotin mAbs. Although bound PrP was detected by fluorochrome-coupled mAbs directed against different PrP epitopes than the bead mAb, no immunoreactivity of bound PrP was observed when the fluorochrome-coupled antibody (X-axis) was identical to the bead mAb, suggesting that additional molecules of PrP were not recruited to the misfolded PrP (Fig. 4a; only 8B4 bead-induced PrP misfolding is shown). We have also found that, similar to bead-bound mAb, soluble PrP-BCD mAbs induced PrP misfolding as detected by 4C2 immunoprecipitation, in comparison to uncoupled magnetic beads, and beads coupled to BSA (Fig. 4b). The immunoprecipitated misfolded PrP was not resistant to PK digestion (Fig. 4b; only 8B4- and 6D11-induced misfolding are shown). Thus,

the bityrosine exposure induced by physical contact with PrP-BCD mAbs is not accompanied by dissociation of the PrP^C β -sheet, nor template generation or protease resistance, which are characteristics of PrP^{Sc}.

Discussion

Conversion of PrP^C to the abnormal β -sheet-rich, PK-resistant isoform (generically designated as PrP^{Sc}) is thought to occur by a protein-only template-directed conversion. However, the mechanics of this process are almost entirely unknown. We have hypothesized that PrP conversion in disease may comprise three steps: (i) binding of PrP^C to PrP^{Sc} via PrP binding and conversion domains; (ii) partial unfolding of PrP (including dissociation of the short β -sheet), thus enabling sampling of conformation space by part of the previously structured domain; and (iii) conformational selection of nascent PrP^{Sc} molecules by intermolecular backbone interactions with the template. We propose the term ‘demiglobule’ for the intermediate PrP species characterized by regional loss of tertiary structure (i.e. dissociation of the β -sheet) as well as other features of the molten globule state.

We now report a novel approach to elucidate the events in template-directed conversion in a tractable, defined and non-infectious system based on antibody mimicry of the interactions between PrP^{Sc} and PrP^C, as monitored by an mAb reactive with exposed bityrosines. We demonstrate that three mAbs directed against PrP-BCD epitopes—in the N-terminus, the C-terminus and an unstructured region adjoining the 3F4 epitope in hamster and human PrP—can trigger partial denaturation of the structured domain of PrP^C, with exposure of bityrosines in α -helices 1 and 3. We interpret bityrosine mAb binding to these regions to be reporting on structural loosening of these regions, which then resemble the free peptide against which the YYR antibodies were raised and screened (Paramithiotis *et al.*, 2003). We also speculate that this loss of structure is not confined to the bityrosine epitopes recognized by 4C2, but specific probes to assess this notion are unavailable. Given the lack of acquisition of protease resistance and recruiting activity, we

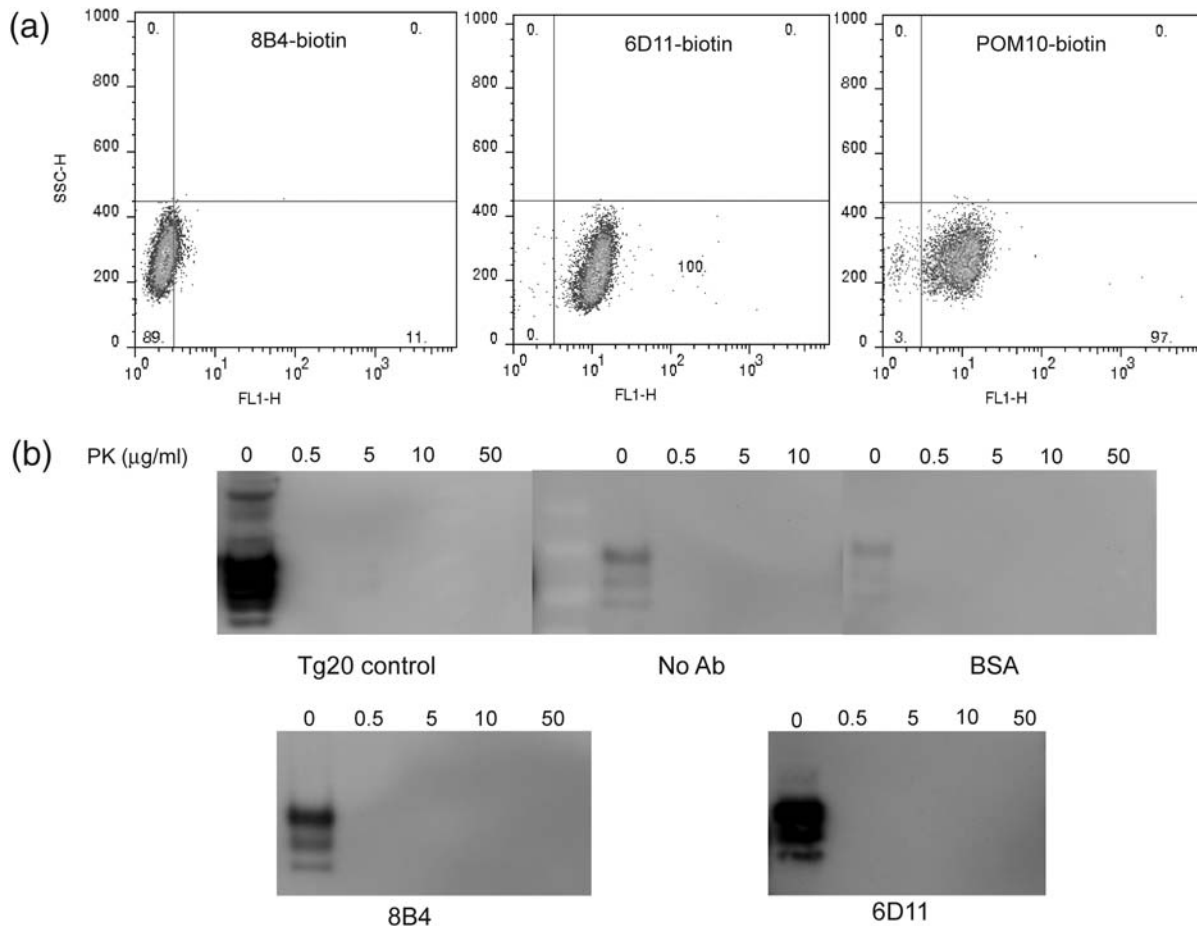


Fig. 4. Induction of bityrosine motifs is not accompanied by other properties of PrP^{Sc}. (a) Induction of Tg20 brain PrP^C by BCD mAbs is not accompanied by recruitment of additional molecules to bound misfolded PrP, as shown by the lack of epitope immunoreactivity identical to the bead BCD (also see Fig. 2a), but preserved immunoreactivity for other PrP epitopes. (b) Immunoprecipitation-immunoblot analysis showing incubation of soluble PrP-BCD with Tg20 brain PrP^C induces bityrosine immunoreactivity, but not PK resistance. Tg20 control is no BCD mAb beads control.

believe that PrP-BCD mAbs do not induce PrP molecular species which are competent to template isoform conversion, i.e. fully infectious PrP^{Sc}. However, early stages in PrP conversion, such as initial structural loosening of PrP^C, may be recapitulated in our system.

The PrP-BCD mAb-induced loss of structure does not include dissociation of the PrP^C β -sheet, as shown by competition experiments and lack of reactivity with β -strand-specific antibodies. An estimation of the energy barrier to exposure of the three bityrosine motifs is consistent with our data, showing β -sheet dissociation exposing β -strand 2 to be much less probable than loss of structure of the bityrosines in α -helix 1 and at the C-terminus (Table I). These estimations were based on the NMR structure of PrP^C and were determined by separate calculation of unfolding solvation entropy, configurational entropy, enthalpy and electrostatic effects (Guest *et al.*, 2008). Both the α -helix 1 YYR and C-terminus YY display relatively low stabilizing energy, whereas the high free energy cost of exposure for β -sheet 2 YYR may prohibit antibody access of this bityrosine motif following PrP-BCD mAb induction.

In this study, it was observed that antibody binding to regions in the unstructured N-terminal domain of PrP^C can induce conformational change in the structured domain of PrP^C. A possible explanation for this seeming ‘action at a

Table I. Energy of exposure for YY(R) motifs following antibody binding

Residues	Location	Sequence	Energy of exposure
149–151	First α -helix	YYR	8 kcal/mol
162–164	Second β -strand	YYR	15 kcal/mol
225–228	C-terminus	YYQR	2 kcal/mol

distance’ is that the N-terminal domain, despite an apparent lack of structure in NMR studies, associates with the structured domain in a way that is essentially invisible to NMR. Incubation of recombinant human PrP with 8B4 or another N-terminal reactive PrP mAb block accessibility of a C-terminal PrP epitope, consistent with such an interaction (Li *et al.*, 2000). Further findings in support of this hypothesis are available from solved NMR structures of PrP^C with varying lengths of the N-terminal unstructured domain (Zahn *et al.*, 2000). Differences in RMS fluctuations among the members of each ensemble indicate that the unstructured domain does play a role in stabilizing some regions more than others, even though the average structure is minimally affected by domain length (Fig. 5). Interestingly, one of the regions of PrP^C with the greatest change in RMS fluctuations due to the unstructured domain coincides with the location

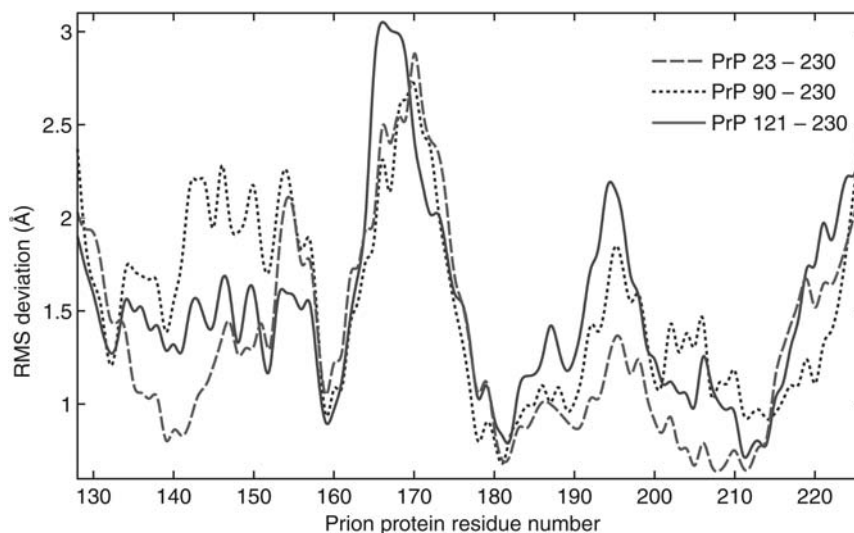


Fig. 5. Root-mean-square deviations of residues in prion protein of various lengths as previously reported (Zahn *et al.*, 2000). A five-residue smoothing window has been applied. The structural ensemble data for PrP 23–230 (structured domain with full N-terminal tail) are taken from PDB file 1QLZ; data for PrP 90–230 (structured domain with partial N-terminal tail) are taken from 1QM1; and data for PrP 121–230 (only structured domain) are taken from 1QM3.

of the bityrosine residues in α -helix 1. This association is perhaps favored by a range of transient contacts between the unstructured domain and surface residues of the folded domain, so that a single fixed set of native stabilizing contacts between them does not exist. Such an ‘avidity enhanced structure’ may explain this domain’s ability to reduce the fluctuations and enhance the stability of specific regions of the folded domain, despite the fact that it lacks a single defined fold.

Funding

This work was supported by PrioNet Canada, a Networks of Centres of Excellence funded by the Government of Canada, and Canadian Institutes of Health Research, the Natural Sciences and Engineering Research Council, the A.P. Sloan Foundation and the Michael Smith Foundation for Health Research.

References

- Alonso,D.O., DeArmond,S.J., Cohen,F.E. and Daggett,V. (2001) *Proc. Natl Acad. Sci. USA*, **98**, 2985–2989.
- Atarashi,R., Moore,R.A., Sim,V.L., Hughson,A.G., Dorward,D.W., Onwubiko,H.A., Priola,S.A. and Caughey,B. (2007) *Nat. Methods*, **4**, 645–650.
- Bessen,R.A., Kocisko,D.A., Raymond,G.J., Nandan,S., Lansbury,P.T. and Caughey,B. (1995) *Nature*, **375**, 698–700.
- Caughey,B.W., Dong,A., Bhat,K.S., Ernst,D., Hayes,S.F. and Caughey,W.S. (1991) *Biochemistry*, **30**, 7672–7680.
- Caughey,B., Kocisko,D.A., Raymond,G.J. and Lansbury,P.T. Jr (1995) *Chem. Biol.*, **2**, 807–817.
- Caughey,B., Raymond,G.J., Kocisko,D.A. and Lansbury,P.T. Jr (1997) *J. Virol.*, **71**, 4107–4110.
- Chabry,J., Caughey,B. and Chesebro,B. (1998) *J. Biol. Chem.*, **273**, 13203–13207.
- Chabry,J., Priola,S.A., Wehrly,K., Nishio,J., Hope,J. and Chesebro,B. (1999) *J. Virol.*, **73**, 6245–6250.
- DeMarco,M.L. and Daggett,V. (2004) *Proc. Natl Acad. Sci. USA*, **101**, 2293–2298.
- DeMarco,M.L. and Daggett,V. (2007) *Biochemistry*, **46**, 3045–3054.
- DeMarco,M.L., Silveira,J., Caughey,B. and Daggett,V. (2006) *Biochemistry*, **45**, 15573–15582.
- Enari,M., Flechsig,E. and Weissmann,C. (2001) *Proc. Natl Acad. Sci. USA*, **98**, 9295–9299.
- Fischer,M., Rulicke,T., Raeber,A., Sailer,A., Moser,M., Oesch,B., Brandner,S., Aguzzi,A. and Weissmann,C. (1996) *EMBO J.*, **15**, 1255–1264.
- Govaerts,C., Wille,H., Prusiner,S.B. and Cohen,F.E. (2004) *Proc. Natl Acad. Sci. USA*, **101**, 8342–8347.
- Griffith,J.S. (1967) *Nature*, **215**, 1043–1044.
- Guest,W., Cashman,N.R. and Plotkin,S.S. (2008) An estimate of PrPc beta sheet dissociation gibbs free energy: implications for prion conversion. *Prion 2008 Conference, 8–10 October; Madrid.*
- Heppner,F.L., Musahl,C., Arrighi,I., Klein,M.A., Rulicke,T., Oesch,B., Zinkernagel,R.M., Kalinke,U. and Aguzzi,A. (2001) *Science*, **294**, 178–182.
- Horiuchi,M. and Caughey,B. (1999) *EMBO J.*, **18**, 3193–3203.
- Horiuchi,M., Baron,G.S., Xiong,L.W. and Caughey,B. (2001) *J. Biol. Chem.*, **276**, 15489–15497.
- Kocisko,D.A., Come,J.H., Priola,S.A., Chesebro,B., Raymond,G.J., Lansbury,P.T. and Caughey,B. (1994) *Nature*, **370**, 471–474.
- Korth,C., *et al.* (1997) *Nature*, **390**, 74–77.
- Li,R., Liu,T., Wong,B.S., Pan,T., Morillas,M., Swietnicki,W., O’Rourke,K., Gambetti,P., Surewicz,W.K. and Sy,M.S. (2000) *J. Mol. Biol.*, **301**, 567–573.
- Li,L., Coulthart,M.B., Balachandran,A., Chakrabarty,A. and Cashman,N.R. (2007) *Biochem. Biophys. Res. Commun.*, **364**, 796–800.
- Merz,P.A., Somerville,R.A., Wisniewski,H.M. and Iqbal,K. (1981) *Acta Neuropathol.*, **54**, 63–74.
- Merz,P.A., Somerville,R.A., Wisniewski,H.M., Manuelidis,L. and Manuelidis,E.E. (1983) *Nature*, **306**, 474–476.
- Meyer,R.K., McKinley,M.P., Bowman,K.A., Braunfeld,M.B., Barry,R.A. and Prusiner,S.B. (1986) *Proc. Natl Acad. Sci. USA*, **83**, 2310–2314.
- Moroncini,G., Kanu,N., Solfrosi,L., Abalos,G., Telling,G.C., Head,M., Ironside,J., Brookes,J.P., Burton,D.R. and Williamson,R.A. (2004) *Proc. Natl Acad. Sci. USA*, **101**, 10404–10409.
- Mouillet-Richard,S., Ermonval,M., Chebassier,C., Laplanche,J.L., Lehmann,S., Launay,J.M. and Kellermann,O. (2000) *Science*, **289**, 1925–1928.
- Pan,K.M., *et al.* (1993) *Proc. Natl Acad. Sci. USA*, **90**, 10962–10966.
- Pan,T., Li,R., Kang,S.C., Wong,B.S., Wisniewski,T. and Sy,M.S. (2004) *J. Neurochem.*, **90**, 1205–1217.
- Pankiewicz,J., Prelli,F., Sy,M.S., Kascak,R.J., Kascak,R.B., Spinner,D.S., Carp,R.I., Meeker,H.C., Sadowski,M. and Wisniewski,T. (2006) *Eur. J. Neurosci.*, **23**, 2635–2647.
- Paramithiotis,E., *et al.* (2003) *Nat. Med.*, **9**, 893–899.
- Peretz,D., *et al.* (2001) *Nature*, **412**, 739–743.
- Polymenidou,M., Stoeck,K., Glatzel,M., Vey,M., Bellon,A. and Aguzzi,A. (2005) *Lancet Neurol.*, **4**, 805–814.
- Prusiner,S.B. (1982) *Science*, **216**, 136–144.
- Prusiner,S.B. (1998) *Proc. Natl Acad. Sci. USA*, **95**, 13363–13383.

- Prusiner,S.B., McKinley,M.P., Bowman,K.A., Bolton,D.C., Bendheim,P.E., Groth,D.F. and Glenner,G.G. (1983) *Cell*, **35**, 349–358.
- Riesner,D., Kellings,K., Wiese,U., Wulfert,M., Mirenda,C. and Prusiner,S.B. (1993) *Dev. Biol. Stand.*, **80**, 173–181.
- Saborio,G.P., Permanne,B. and Soto,C. (2001) *Nature*, **411**, 810–813.
- Safar,J., Roller,P.P., Gajdusek,D.C. and Gibbs,C.J. Jr (1993) *J. Biol. Chem.*, **268**, 20276–20284.
- Sassoon,J., Sadowski,M., Wisniewski,T. and Brown,D.R. (2005) *Mini Rev. Med. Chem.*, **5**, 361–366.
- Solforosi,L., Bellon,A., Schaller,M., Cruite,J.T., Abalos,G.C. and Williamson,R.A. (2007) *J. Biol. Chem.*, **282**, 7465–7471.
- Wille,H., Michelitsch,M.D., Guenebaut,V., Supattapone,S., Serban,A., Cohen,F.E., Agard,D.A. and Prusiner,S.B. (2002) *Proc. Natl Acad. Sci. USA*, **99**, 3563–3568.
- Wille,H., Govaerts,C., Borovinskiy,A., Latawiec,D., Downing,K.H., Cohen,F.E. and Prusiner,S.B. (2007) *Arch. Biochem. Biophys.*, **467**, 239–248.
- Zahn,R., Liu,A., Luhrs,T., Riek,R., Von Schroetter,C., Garcia,F.L., Billeter,M., Calzolari,L., Wider,G. and Wuthrich,K. (2000) *Proc. Natl. Acad. Sci. USA*, **97**, 145–150.
- Zou,W.Q. and Cashman,N.R. (2002) *J. Biol. Chem.*, **277**, 43942–43947.

**Received June 7, 2009; revised June 7, 2009;
accepted June 11, 2009**

Edited by Byron Caughey